

See discussions, stats, and author profiles for this publication at: <https://www.researchgate.net/publication/260266778>

Deciphering Chemical Bonding in a BC₃ Honeycomb Epitaxial Sheet

ARTICLE *in* THE JOURNAL OF PHYSICAL CHEMISTRY C · JANUARY 2012

Impact Factor: 4.77 · DOI: 10.1021/jp210956w

CITATIONS

25

READS

39

2 AUTHORS:



Ivan A. Popov

Utah State University

35 PUBLICATIONS 237 CITATIONS

[SEE PROFILE](#)



Alexander I. Boldyrev

Utah State University

341 PUBLICATIONS 9,920 CITATIONS

[SEE PROFILE](#)

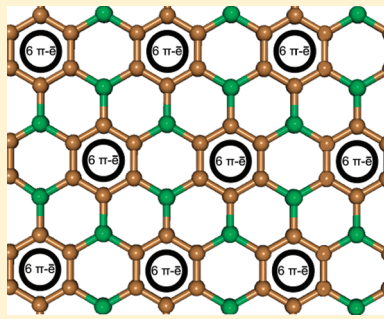
Deciphering Chemical Bonding in a BC₃ Honeycomb Epitaxial Sheet

Ivan A. Popov and Alexander I. Boldyrev*

Department of Chemistry and Biochemistry, Utah State University, 0300 Old Main Hill, Logan, Utah 84322, United States

S Supporting Information

ABSTRACT: The substitution of every fourth carbon atom in graphene by a boron atom preserves the honeycomb structure in the BC₃ two-dimensional lattice, but as we found in our adaptive natural density partitioning analysis, it remarkably alters the chemical bonding. First, in the BC₃ lattice, where boron atoms are surrounded by three carbon atoms, carbon forces boron to form two-center–two-electron B–C σ -bonds, while boron is known to participate only in multicenter (three-center–two-electron or four-center–two-electron) σ -bonding in the most stable two-dimensional form of the pure boron lattice, the α -sheet. Second, six-center–two-electron π -bonds found over every hexagon in graphene and in the α -sheet migrate in BC₃ to hexagons composed out of carbon atoms only, making π -bonding in those hexagons more similar to the corresponding π -bonding in benzene rather than graphene, leaving hexagons formed by carbon and boron atoms in the BC₃ lattice empty without π -bonding. We believe that chemical bonding elements found in our chemical bonding analysis of graphene, the α -sheet of boron, and the BC₃ lattice will be useful tools for rationalizing chemical bonding in other two-dimensional boron–carbon materials.



INTRODUCTION

Pure boron^{1–4} and boron–carbon^{5–13} two-dimensional materials have gained significant attention since the discovery of graphene.^{14,15} The isolated layers of graphene were found to have many unusual properties such as high carrier mobilities ($>200\,000\text{ cm}^2\text{V}^{-1}\text{s}^{-1}$ at electron densities of $2 \times 10^{11}\text{ cm}^{-2}$),^{16–19} exceptional Young modulus values ($>0.5\text{--}1\text{ TPa}$), and large force constants ($1\text{--}5\text{ N m}^{-1}$).^{20–22} Due to these properties graphene is attractive for many potential commercial applications such as energy storage²³ and micro- and optoelectronics.²⁴ There is no doubt that other two-dimensional materials have a great potential for nanotechnology as much as graphene.

Understanding chemical bonding in these two-dimensional materials is crucial for rationalizing different kinds of defects such as point defects, single, double, and multiple vacancies, foreign adatoms, substitutional impurities,²⁵ and new materials that are their derivatives. In our previous studies we analyzed chemical bonding in graphene²⁶ and the most stable form of two-dimensional boron, the so-called α -sheet.⁴ According to our analysis, σ -bonding in graphene is built out of two-center–two-electron (2c–2e) C–C σ -bonds, making the graphene honeycomb structure very rigid. The π -bonding in graphene is very different from the corresponding π -bonding in benzene, coronene, or other polycyclic hydrocarbons, because aromaticity in graphene is local with one pair of π -electrons located over every hexagon. The chemical bonding in the α -sheet is also very different from that of graphene.

The α -sheet structure is built out of filled and empty hexagons.^{1–3} According to our analysis, there are three 3c–2e σ -bonds in every filled hexagon which border the holes, three 4c–2e σ -bonds at the junction of two filled hexagons, one 7c–2e π -bond delocalized over the filled hexagon, and one 6c–2e

π -bond delocalized over the empty hexagon, so in total, there are eleven electrons participating in the formation of chemical bonding of the filled hexagon: six valence electrons coming from the three 3c–2e σ -bonds, three valence electrons coming from the three 4c–2e σ -bonds, and two electrons coming from the 7c–2e π -bond. On the other hand, the filled hexagon, considered as a part of the lattice, should have nine valence electrons coming from the six peripheral boron atoms and three valence electrons coming from the central atom, resulting in twelve electrons per filled hexagon. Thus, there is one extra electron on each filled hexagon motif not involved in the bonding presented above. This extra electron is involved in formation of the 6c–2e π -bond over the empty hexagons. Therefore, the α -sheet structure needs those empty hexagons as scavengers of extra electrons from the filled hexagons. In contrast to graphene, which contains 2c–2e C–C σ -bonds, the all-boron α -sheet possesses no localized 2c–2e B–B σ -bonds.

These two different chemical bonding pictures presented for graphene and the α -sheet raise the following question: What kind of chemical bonding can one expect in two-dimensional carbon–boron lattices? In this paper we present our analysis of chemical bonding in a BC₃ honeycomb sheet, based on the experimental structure presented in Figure 1, which was determined by low-energy electron diffraction.⁷

THEORETICAL METHODS

Chemical bonding analysis of a BC₃ honeycomb sheet was performed using the fragmental approach and adaptive natural density partitioning (AdNDP) method recently developed by

Received: November 14, 2011

Revised: December 24, 2011

Published: January 5, 2012



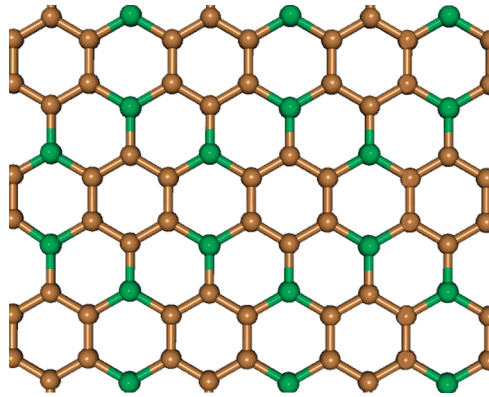


Figure 1. Atomic arrangement in the layer of BC_3 . The green atom is B, and the brown atom is C.

Zubarev and Boldyrev,²⁷ AdNDP initially searches for core electron pairs and lone pairs ($1\text{c}-2\text{e}$), then $2\text{c}-2\text{e}$, $3\text{c}-2\text{e}$, ..., and finally $n\text{c}-2\text{e}$ bonds if necessary. At every step the density matrix is depleted of the density corresponding to the appropriate bonding elements. The user-directed form of the AdNDP analysis can be applied to specified molecular fragments and is analogous to the directed search option of the standard natural bond orbital (NBO) code.^{28,29} AdNDP accepts only those bonding elements whose occupation numbers (ONs) exceed the specified threshold values, which are usually chosen to be close to 2.00 lel. The AdNDP method recovers both Lewis bonding elements ($1\text{c}-2\text{e}$ and $2\text{c}-2\text{e}$ objects, corresponding to the core electrons and lone pairs, and $2\text{c}-2\text{e}$ bonds) and delocalized bonding elements, which are associated with the concepts of aromaticity and antiaromaticity. We used a hybrid density functional method known in the literature as B3LYP^{30,31} and the 6-31G basis set³² for the AdNDP calculations. Geometry optimization and frequency calculations for the model fragments $\text{B}_6\text{C}_6\text{H}_{12}$, $\text{B}_{10}\text{C}_{12}\text{H}_{18}$, and $\text{B}_{16}\text{C}_{24}\text{H}_{24}$ were performed using the B3LYP/cc-pvTZ^{33,34} level of theory. To assess the aromaticity of different rings in these fragments, we calculated nucleus independent chemical shift (NICS) indices.^{35,36} The AdNDP calculations were performed using the AdNDP program written by Zubarev.²⁷ All density functional theory (DFT) calculations were done using the Gaussian 03 software package.³⁷ Molecular visualization was performed using Molekel 5.4.0.8.³⁸

RESULTS AND DISCUSSION

Our first $\text{B}_6\text{C}_6\text{H}_{12}$ fragment is shown in Figure 2 as structure II. This is the smallest fragment where we believe the chemical bonding in the infinite lattice is primarily preserved. Bonds

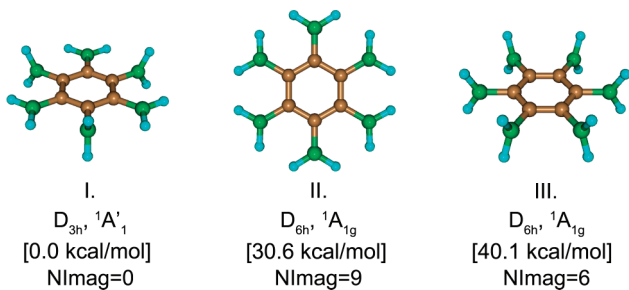


Figure 2. $\text{B}_6\text{C}_6\text{H}_{12}$ molecular structures. The green atom is B, the brown atom is C, and the blue atom is H.

between boron and carbon atoms in the extended honeycomb sheet, shown in Figure 1, are substituted by B–H σ -bonds, which as we will see do not disturb much the chemical bonding in the fragment compared to the infinite sheet. Since our fragment is also a regular molecule, we performed geometry optimization and frequency calculations for structures I–III at the B3LYP/cc-pvTZ level of theory. Our fragment structure II is in fact a ninth-order saddle point. Geometry optimization following the imaginary frequencies led us to structure I, which is the most stable isomer found in our calculations. Even though structure II is not even a local minimum, we believe that it represents the correct chemical bonding pattern in the infinite BC_3 lattice. Our calculated $R(\text{C}-\text{C}) = 1.43 \text{ \AA}$ bond and $R(\text{B}-\text{C}) = 1.58 \text{ \AA}$ (at B3LYP/cc-pvTZ) are very close to the experimental values of $R(\text{C}-\text{C}) = 1.42 \text{ \AA}$ and $R(\text{B}-\text{C}) = 1.55 \text{ \AA}$.⁷ The optimized $R(\text{C}-\text{C})$ bond is about the same in all three structures, but the optimized $R(\text{B}-\text{C})$ bond varies from 1.52 to 1.58 \AA . We also mention that structure II, which serves as the model fragment, is about 30 kcal/mol higher in energy than structure I, showing that the BC_3 lattice, presented in Figure 1, has some strain energy even though it was shown to be the most stable form for this stoichiometry.⁹ We believe that the reason why structure II is not a minimum is the repulsion between terminal hydrogen atoms. To test that, we first optimized the geometries and calculated the frequencies of two molecules: $1,2\text{-C}_6\text{H}_4(\text{BH}_2)_2$ and $1,3\text{-C}_6\text{H}_4(\text{BH}_2)_2$. We found that both of these molecules are completely planar in the most stable configuration. Apparently, repulsion between just two H atoms is not enough to overcome stabilization due to conjugation of the π -system of C_6 with empty orbitals of boron. We next calculated $1,2,3\text{-C}_6\text{H}_4(\text{BH}_2)_2$ and $1,3,5\text{-C}_6\text{H}_4(\text{BH}_2)_2$. The $1,3,5\text{-C}_6\text{H}_4(\text{BH}_2)_2$ molecule is most stable when it is completely planar, but in this case the BH_2 groups are well separated from each other. However, the completely planar structure of the $1,2,3\text{-C}_6\text{H}_4(\text{BH}_2)_2$ molecule has two imaginary frequencies. Thus, we proved that the repulsion between hydrogen atoms is responsible for the instability of isomer II in the $\text{C}_6(\text{BH}_2)_6$ case.

The results of the AdNDP analysis for the $\text{B}_6\text{C}_6\text{H}_{12}$ fragment are shown in Figure 3. Our analysis revealed six $2\text{c}-2\text{e}$ C–C σ -bonds, six $2\text{c}-2\text{e}$ B–C σ -bonds, and twelve $2\text{c}-2\text{e}$ B–H σ -bonds, which all have ON values that are close to the ideal value of 2.00 lel. Thus, σ -bonding in this fragment between boron and carbon atoms as well as between carbon atoms is very similar to that of graphene in a sense that these bonds are $2\text{c}-2\text{e}$. According to the AdNDP analysis, there are three $6\text{c}-2\text{e}$ π -bonds which are very similar to those of benzene,³⁹ which is not surprising since our fragment is a derivative of benzene. However, we point out that our ON values of π -bonds (1.75 and 1.89 lel) in the fragment are appreciably lower than the ON values of π -bonds (2.00 lel) in benzene. The deviation of the ON values of π -bonds from 2.00 lel in this fragment indicates that these bonds tend to be delocalized over a larger number of atoms than six. Indeed, when we performed the direct search for the π -bonding on twelve atoms including both carbon and boron atoms, we obtained ON values of 2.00 lel for all the π -bonds. Thus, the difference between $6\text{c}-2\text{e}$ and $12\text{c}-2\text{e}$ bonds is due to the participation of $2p_z$ atomic orbitals (AOs) of boron in π -bonding, which turned out to be 0.10 lel per boron atom. The degree of the participation of boron atoms in π -bonding can also be evaluated from the NBO analysis of structures II and III since delocalization of π -bonding toward boron atoms is possible in structure II, but not possible in

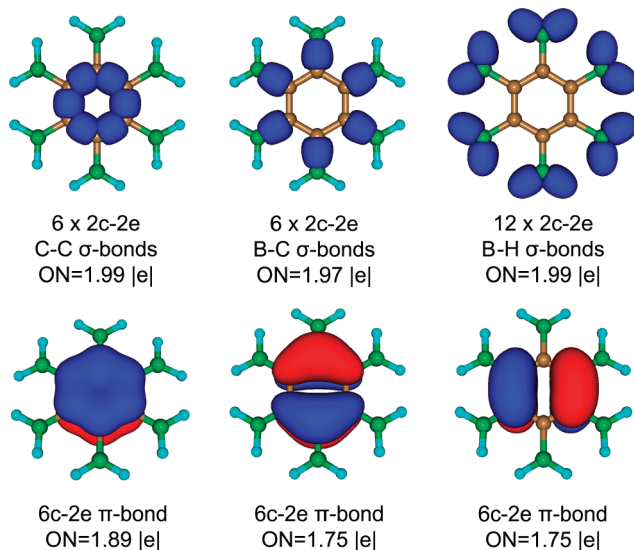


Figure 3. Chemical bonds revealed by the AdNDP analysis at the B3LYP/6-31G//B3LYP/cc-pvTZ level of theory.

structure III. According to our NBO analysis, we found that the boron atom in structure II has the higher occupation number of $2p_z$ AOs by 0.06 lel than the boron atom in structure III. This result is consistent with our AdNDP analysis.

Since our analysis and the B3LYP method both work well if the wave function is essentially one-configurational, we performed single-point CASSCF(14,15)/6-31G calculations. According to these results, the Hartree–Fock configuration has a 0.964 coefficient out of a total of 20 707 830 configurations, thus confirming that our wave function is primarily one-configurational and our analysis is valid.

Our second $B_{10}C_{12}H_{18}$ fragment is presented in Figure 4. The second fragment allows us to see how two boron atoms are affected by two carbon hexagons at the junction. Optimized $R(B-C)$ and $R(C-C)$ were found to be 1.57 and 1.42–1.44 Å, respectively, which are in good agreement with the experimental data. The AdNDP analysis revealed that all σ -bonds are classical 2c–2e bonds with the ON very close to 2.00 lel. We found a set of three π -bonds delocalized over every carbon hexagon with about the same ON as in the $B_6C_6H_{12}$

fragment, which is also an indication of some participation of boron atoms in the π -bonding.

Results obtained at the CASSCF(10,10)/6-31G level of theory indicate that the wave function of this model fragment is also one-configurational: the first coefficient in the expansion of the wave function equals 0.926 (the total number of configurations is 31 878).

Our third $B_{16}C_{24}H_{24}$ fragment is shown in Figure 5. The third fragment is essentially a tetramer of the first fragment, and it contains four carbon hexagons and two boron atoms at the center with the surrounding atoms, which they would have in the infinite BC_3 lattice. The optimized $R(B-C)$ and $R(C-C)$ were found to be 1.56–1.58 and 1.41–1.43 Å, respectively, which are again in good agreement with the experimental data for the lattice. As in the first two fragments all σ -bonds are classical with the ON close to 2.00 lel. We found a set of three π -bonds delocalized over every carbon hexagon with about the same ON as in the $B_6C_6H_{12}$ fragment, which also is an indication of some participation of boron atoms in the π -bonding. To test the chemical bonding picture recovered by the AdNDP method, we also performed NBO analysis at the B3LYP/6-31G//B3LYP/cc-pvTZ level of theory for the three fragments. Results of this analysis are presented in Figure 6.

Like in the AdNDP, the NBO analysis revealed that σ -bonding is classical, with the ON values varying between 1.96 and 1.99 lel. As for the π -bonding, the NBO analysis produced one of the Kekulé structures with three alternate double C–C bonds in each carbon hexagon. Thus, the NBO analysis confirmed the presence of aromatic benzene-like carbon hexagons in all the studied fragments. The low ON values of these double bonds also indicate their tendency to be delocalized.

To investigate aromaticity further, we calculated NICS and $NICS_{zz}$ indices over all the hexagons labeled in Figures 4 and 5 as A, B, C, and D. NICS and $NICS_{zz}$ indices were calculated over the center of those hexagons at the z coordinates from $z = 0.0$ Å to $z = 2.0$ Å with an interval of 0.5 Å. Results of these calculations are summarized in Table 1.

To have reference points, we also calculated NICS and $NICS_{zz}$ indices for the prototypical aromatic molecule benzene at the same level of theory. Results of these calculations are summarized in Table S1 in the Supporting Information. Negative values of NICS and $NICS_{zz}$ indicate the presence of aromaticity, while positive ones show the presence of

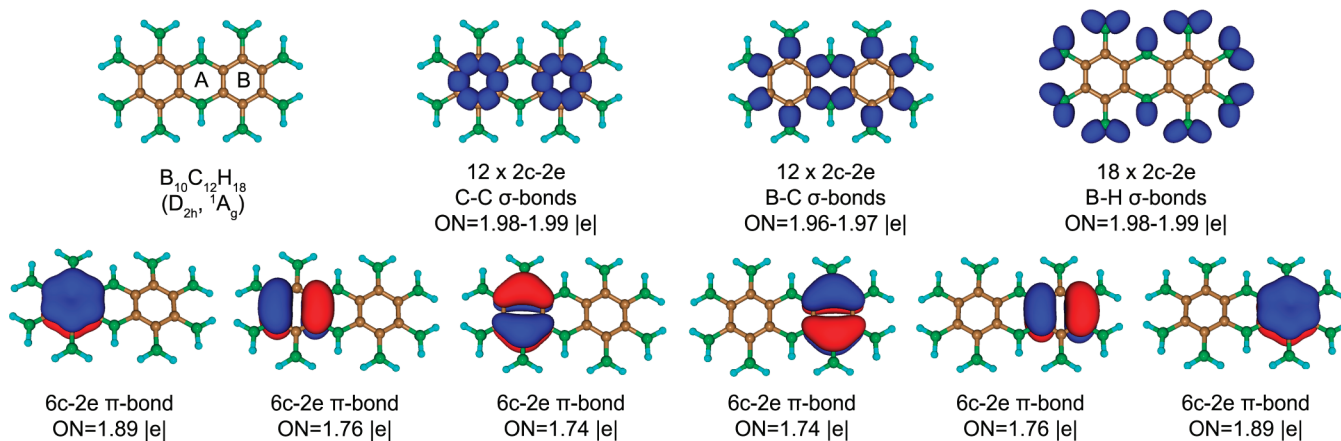


Figure 4. Structure and chemical bonds of the $B_{10}C_{12}H_{18}$ fragment revealed by the AdNDP analysis at the B3LYP/6-31G//B3LYP/cc-pvTZ level of theory.

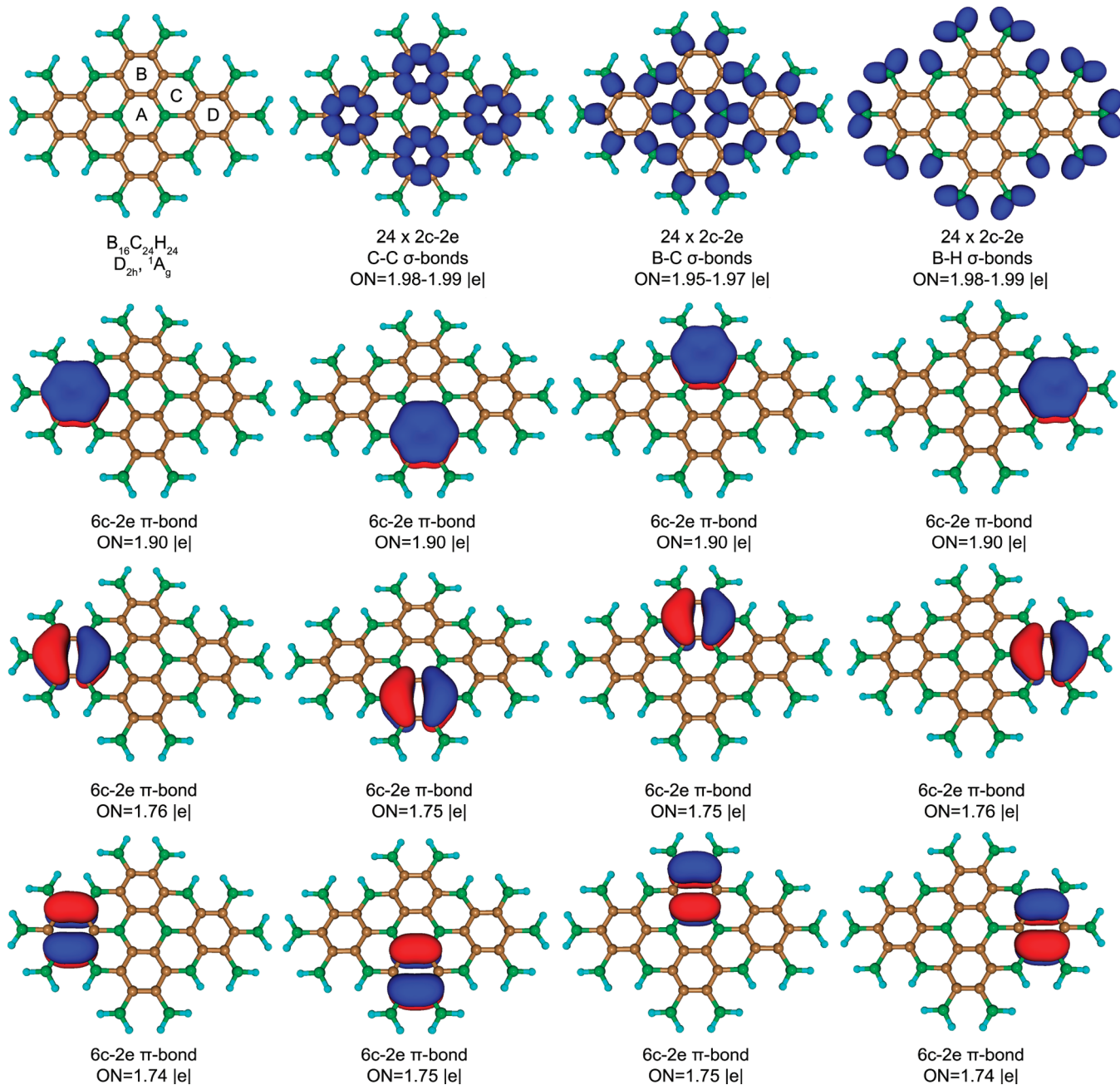


Figure 5. Structure and chemical bonds of the $B_{16}C_{24}H_{24}$ fragment revealed by the AdNDP analysis at the B3LYP/6-31G//B3LYP/cc-pvTZ level of theory.

antiaromaticity.^{35,36} No matter what indices, NICS or NICS_{zz}, we considered, we found for the $B_{10}C_{12}H_{18}$ and $B_{16}C_{24}H_{24}$ fragments that hexagons (B and D) composed out of carbon atoms are aromatic while hexagons (A and C) composed out of carbon and boron atoms are antiaromatic. As for the $B_6C_6H_{12}$ fragment, both NICS and NICS_{zz} indices also show an aromatic picture for the C_6 ring though the values of NICS and NICS_{zz} are somewhat lower than those in benzene. Thus, the overall chemical bonding picture revealed by the AdNDP, NBO, NICS, and NICS_{zz} analyses is consistent. The one-configurational nature of the fragment wave function was confirmed at the CASSCF(8,8)/6-31G level of theory: the first coefficient in the expansion of the wave function is found to be 0.929 (the total number of configurations is 1764).

CONCLUSION

The chemical bonding analysis performed for the BC_3 lattice revealed a chemical bonding picture very different from the corresponding one in graphene and the all-boron α -sheet. We found that the σ -bonding in BC_3 is classical, composed out of 2c-2e B-C and C-C bonds, reminiscent of that in graphene. Thus, carbon forces boron to form 2c-2e σ -bonds, in contrast with an all-boron α -sheet, where boron participates only in multicenter (3c-2e or 4c-2e) σ -bonding. However, in contrast with graphene, where there is one 6c-2e π -bond located over every hexagon, in the BC_3 lattice we have six π -electrons located over every carbon hexagon and there are no π -bonds over the hexagons which are composed out of boron and carbon atoms. Moreover, NICS and NICS_{zz} values indicate the presence of antiaromaticity in those hexagons. Thus, 6c-2e π -

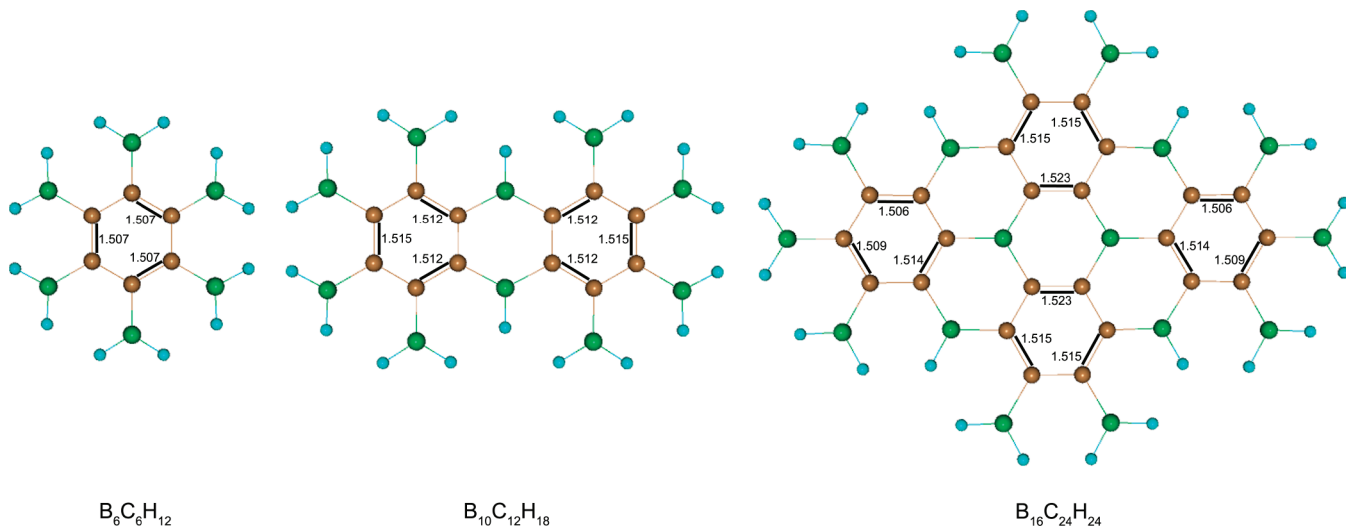


Figure 6. Kekulé structures for the $B_6C_6H_{12}$, $B_{10}C_{12}H_{18}$, and $B_{16}C_{24}H_{24}$ fragments found by the NBO analysis.

Table 1. Calculated NICS and $NICS_{zz}$ Values (ppm) at Different z Coordinates for $B_6C_6H_{12}$, $B_{10}C_{12}H_{18}$, and $B_{16}C_{24}H_{24}$ Fragments at the B3LYP/cc-pvTZ//B3LYP/cc-pvTZ Level of Theory

| fragment | ring label | $R_z^a = 0.0 \text{ \AA}$ | $R_z^a = 0.5 \text{ \AA}$ | $R_z^a = 1.0 \text{ \AA}$ | $R_z^a = 1.5 \text{ \AA}$ | $R_z^a = 2.0 \text{ \AA}$ |
|----------------------|------------|---------------------------|---------------------------|---------------------------|---------------------------|---------------------------|
| $B_6C_6H_{12}$ | A | -3.25 | -6.45 | -9.02 | -7.81 | -5.61 |
| | A^b | -5.50 | -14.98 | -24.29 | -22.69 | -17.27 |
| $B_{10}C_{12}H_{18}$ | A | 12.42 | 9.26 | 4.19 | 1.03 | -0.44 |
| | A^b | 36.01 | 30.01 | 16.36 | 4.86 | -1.11 |
| | B | -1.54 | -4.77 | -7.57 | -6.74 | -4.88 |
| | B^b | -0.41 | -9.94 | -19.98 | -19.50 | -15.03 |
| $B_{16}C_{24}H_{24}$ | A | 11.61 | 8.49 | 3.71 | 0.97 | -0.25 |
| | A^b | 34.51 | 27.98 | 14.55 | 4.24 | -0.84 |
| | B | 0.61 | -2.70 | -5.80 | -5.40 | -3.94 |
| | B^b | 6.20 | -3.55 | -14.58 | -15.44 | -12.11 |
| | C | 11.94 | 8.77 | 3.87 | 1.00 | -0.29 |
| | C^b | 35.16 | 28.81 | 15.27 | 4.51 | -0.89 |
| | D | -0.61 | -3.89 | -6.81 | -6.15 | -4.45 |
| | D^b | 2.46 | -7.20 | -17.63 | -17.65 | -13.64 |

^aDistance from the hexagon center. ^bNICS_{zz} values.

bonds found over every hexagon in graphene and in the α -sheet migrate to hexagons composed out of carbon atoms only, making π -bonding in those hexagons more similar to the corresponding π -bonding in benzene rather than graphene, leaving hexagons formed by carbon and boron atoms in the BC_3 lattice empty without π -bonding. The presence of boron atoms does not destroy the honeycomb network of σ -bonds in BC_3 , while in a pure boron α -sheet there are no 2c–2e B–B σ -bonds. So far, analyzing the chemical bonding in two-dimensional boron, carbon, and boron–carbon materials, we found the following chemical bonding elements: 2c–2e C–C and B–C σ -bonds, 3c–2e σ -bonds and 4c–2e all-boron σ -bonds, 6c–2e all-carbon and all-boron π -bonds, 7c–2e all-boron π -bonds, and benzene-like π -bonding with six π -electrons located over the all-carbon hexagons. The one-configurational nature of the wave functions of all the fragments studied here is confirmed using the multiconfigurational method CASSCF. We strongly believe that these bonding elements will be important for rationalizing chemical bonding in other boron–carbon two-dimensional materials.

■ ASSOCIATED CONTENT

S Supporting Information

Calculated NICS and $NICS_{zz}$ values (ppm) at different z coordinates for C_6H_6 at the B3LYP/cc-pvTZ//B3LYP/cc-pvTZ level of theory. This material is available free of charge via the Internet at <http://pubs.acs.org>.

■ AUTHOR INFORMATION

Corresponding Author

*E-mail:a.i.boldyrev@usu.edu.

■ ACKNOWLEDGMENTS

The National Science Foundation (Grant CHE-1057746) supported this work. Cluster time and other computational resources from the Center for High Performance Computing at Utah State University are gratefully acknowledged. The computational resources of the 64 node Wasatch cluster were funded by the National Institute of Food and Agriculture, U.S. Department of Agriculture, through the High Performance Computing Utah grant.

■ REFERENCES

- (1) Tang, H.; Ismail-Beigi, S. *Phys. Rev. Lett.* **2007**, *99*, 115501.
- (2) Tang, H.; Ismail-Beigi, S. *Phys. Rev. B* **2009**, *80*, 134113.
- (3) Yang, X.; Ding, Y.; Ni, J. *Phys. Rev. B* **2008**, *77*, 0414402.
- (4) Galeev, T. R.; Chen, Q.; Guo, J.-C.; Bai, H.; Miao, C.-Q.; Lu, H.-G.; Sergeeva, A. P.; Li, S.-D.; Boldyrev, A. I. *Phys. Chem. Chem. Phys.* **2011**, *13*, 11575.
- (5) Kouveticakis, J.; Kaner, R. B.; Sattler, M. L.; Barlett, N. *J. Chem. Soc., Chem. Commun.* **1986**, 1758.
- (6) Way, B. M.; Dahn, J. R.; Tiedje, T.; Myrtle, K.; Kasrai, M. *Phys. Rev. B* **1992**, *46*, 1697.
- (7) Yanagisawa, H.; Tanaka, T.; Ishida, Y.; Matsue, M.; Rokuta, E.; Otani, S.; Oshima, C. *Phys. Rev. Lett.* **2004**, *93*, 177003–1.
- (8) Tomanek, D.; Wentzcovitch, R. M.; Louie, S. G.; Cohen, M. L. *Phys. Rev. B* **1988**, *37*, 3134.
- (9) Luo, X.; Yang, J.; Liu, H.; Wu, X.; Wang, Y.; Ma, Y.; Wei, S.-H.; Gong, X.; Xiang, H. *J. Am. Chem. Soc.* **2011**, *133*, 16285.
- (10) Wu, X.; Pei, Y.; Zeng, X. C. *Nano Lett.* **2009**, *9*, 1577.
- (11) Yanagisawa, H.; Ishida, Y.; Tanaka, T.; Ueno, A.; Otani, S.; Oshima, C. *Surf. Sci.* **2006**, *600*, 4072.
- (12) Yanagisawa, H.; Tanaka, T.; Ishida, Y.; Matsue, M.; Rokuta, E.; Otani, S.; Oshima, C. *Surf. Interface Anal.* **2005**, *37*, 133.
- (13) Ding, Y.; Wang, Y.; Ni, J.; Shi, L.; Shi, S.; Li, C.; Tang, W. *Nanoscale Res. Lett.* **2011**, *6*, 190.
- (14) Novoselov, K. S.; Geim, A. K.; Morozov, S. V.; Jiang, D.; Zhang, Y.; Dubonos, S. V.; Grigorieva, I. V.; Firsov, A. A. *Science* **2004**, *306*, 666.
- (15) Novoselov, K. S.; Geim, A. K.; Morozov, S. V.; Jiang, D.; Katsnelson, M. I.; Grigorieva, I. V.; Dubonos, S. V.; Firsov, A. A. *Nature* **2005**, *438*, 197.
- (16) Unarunotai, S.; Murata, Y.; Chialvo, C. E.; Mason, N.; Petrov, I.; Nuzzo, R. G.; Moore, J. S.; Rogers, J. A. *Adv. Mater.* **2010**, *22*, 1072.
- (17) Bolotin, K. I.; Sikes, K. J.; Jiang, Z.; Klima, M.; Gudenberg, G.; Hone, J.; Kim, P.; Stormer, H. L. *Solid State Commun.* **2008**, *146*, 351.
- (18) Morozov, S. V.; Novoselov, K. S.; Katsnelson, M. I.; Schedin, F.; Elias, D. C.; Jaszczak, J. A.; Geim, A. K. *Phys. Rev. Lett.* **2008**, *100*, 016602.
- (19) Du, X.; Skachko, I.; Barker, A.; Andrei, E. Y. *Nat. Nanotechnol.* **2008**, *3*, 491.
- (20) Frank, I. W.; Tanenbaum, D. M.; Van der Zanda, A. M.; McEuen, P. L. *J. Vac. Sci. Technol., A* **2007**, *25*, 2558.
- (21) Scarpa, F.; Adhikari, S.; Phani, A. S. *Nanotechnology* **2009**, *20*, 065709.
- (22) Faccio, R.; Denis, P. A.; Pardo, H.; Goyenola, C.; Mombru, A. W. *J. Phys.: Condens. Matter* **2009**, *21*, 285304.
- (23) Stoller, M. D.; Park, S.; Zhu, Y.; An, J.; Ruoff, R. S. *Nano Lett.* **2008**, *8*, 3498.
- (24) Mullen, K.; Rabe, J. P. *Acc. Chem. Res.* **2008**, *41*, 511.
- (25) Banhart, F.; Kotakoski, J.; Krasheninnikov, A. V. *ACS Nano* **2011**, *5*, 26.
- (26) Popov, I. A.; Bozhenko, K. V.; Boldyrev, A. I. *Nano Research* **2012**, DOI: 10.1007/s12274-011-0192-z.
- (27) Zubarev, D. Yu.; Boldyrev, A. I. *Phys. Chem. Chem. Phys.* **2008**, *10*, 5207.
- (28) Foster, J. P.; Weinhold, F. *J. Am. Chem. Soc.* **1980**, *102*, 7211.
- (29) Weinhold, F.; Landis, C. *Valency and Bonding. A Natural Bond Orbital Donor-Acceptor Perspective*; Cambridge University Press: Cambridge, U.K., 2005.
- (30) Becke, A. D. *J. Chem. Phys.* **1993**, *98*, 5648.
- (31) Lee, C.; Yang, W.; Parr, R. G. *Phys. Rev. B* **1988**, *37*, 785.
- (32) Ditchfield, R.; Hehre, W. J.; Pople, J. A. *J. Chem. Phys.* **1971**, *54*, 724.
- (33) Dunning, T. H. Jr. *J. Chem. Phys.* **1989**, *90*, 1007.
- (34) Woon, D. E.; Dunning, T. H. Jr. *J. Chem. Phys.* **1993**, *98*, 1358.
- (35) Schleyer, P. v. R.; Maerker, C.; Dransfeld, A.; Jiao, H. J.; Hommes, N. J. R. v. E. *J. Am. Chem. Soc.* **1996**, *118*, 6317.
- (36) Fallah-Bagher-Shaidaei, H.; Wannere, C. S.; Corminboeuf, C.; Puchta, R.; Schleyer, P. v. R. *Org. Lett.* **2006**, *8*, 863.
- (37) Frisch, M. J.; Trucks, G. W.; Schlegel, H. B.; Scuseria, G. E.; Robb, M. A.; Cheeseman, J. R.; Montgomery, J. A., Jr.; Vreven, T.; Kudin, K. N.; Burant, J. C.; Millam, J. M.; Iyengar, S. S.; Tomasi, J.; Barone, V.; Mennucci, B.; Cossi, M.; Scalmani, G.; Rega, N.; Petersson, G. A.; Nakatsuji, H.; Hada, M.; Ehara, M.; Toyota, K.; Fukuda, R.; Hasegawa, J.; Ishida, M.; Nakajima, T.; Honda, Y.; Kitao, O.; Nakai, H.; Klene, M.; Li, X.; Knox, J. E.; Hratchian, H. P.; Cross, J. B.; Bakken, V.; Adamo, C.; Jaramillo, J.; Gomperts, R.; Stratmann, R. E.; Yazyev, O.; Austin, A. J.; Cammi, R.; Pomelli, C.; Ochterski, J. W.; Ayala, P. Y.; Morokuma, K.; Voth, G. A.; Salvador, P.; Dannenberg, J. J.; Zakrzewski, V. G.; Dapprich, S.; Daniels, A. D.; Strain, M. C.; Farkas, O.; Malick, D. K.; Rabuck, A. D.; Raghavachari, K.; Foresman, J. B.; Ortiz, J. V.; Cui, Q.; Baboul, A. G.; Clifford, S.; Cioslowski, J.; Stefanov, B. B.; Liu, G.; Liashenko, A.; Piskorz, P.; Komaromi, I.; Martin, R. L.; Fox, D. J.; Keith, T.; Al-Laham, M. A.; Peng, C. Y.; Nanayakkara, A.; Challacombe, M.; Gill, P. M. W.; Johnson, B.; Chen, W.; Wong, M. W.; Gonzalez, C.; Pople, J. A. *Gaussian 03*, revision D.01; Gaussian, Inc.: Wallingford, CT, 2004.
- (38) Varetto, U. *Molekel 5.4.0.8*; Swiss National Supercomputing Centre: Manno, Switzerland.
- (39) Zubarev, D. Yu.; Boldyrev, A. I. *J. Org. Chem.* **2008**, *73*, 9251.